

# **Hyperbolic Equations: Finite difference and Mimetic Numerical Schemes**

## **2.2 1D Elasticity Problem - Equations**

Elasticity theory can be used to derive the system of equations that represents a one-dimensional elastic wave propagating in a solid. There are two modes of propagation in a solid, one where the compressional disturbance in the material is produced in the same direction than the propagation of the waves (P-waves)

---

and other where the compressional disturbance is produced orthogonal to the direction of propagation (S-waves). In the one dimensional case, all the quantities vary only in one direction and parallel and orthogonal waves can be decoupled into two independent hyperbolic systems of two equations each. The system:

$$\rho \frac{\partial \nu}{\partial t} = \frac{\partial \sigma}{\partial x} \quad (2)$$

$$\frac{\partial \sigma}{\partial t} = \mu \frac{\partial \nu}{\partial x} \quad (3)$$

corresponds to the equations for a linear S-wave (small deformations are assumed in order that the theory of linear elasticity holds). In this coupled set of equations  $\nu$  stands for velocity,  $\sigma$  for stress, and the constants  $\rho$  and  $\mu$  represent the density of the material and the shear modulus, respectively.

Next, finite difference schemes as well as the mimetic discretization are applied to the system of equations: (2) and (3). For each case, a derivation of the discrete expressions used to calculate the evolution of the system is included.

## 2.3 Finite Difference Schemes

### 2.3.1 Forward Time Central Space (FTCS)

$$\begin{aligned} \rho \frac{\nu_i^{n+1} - \nu_i^n}{\Delta t} &= \frac{\sigma_{i+1}^n - \sigma_{i-1}^n}{2\Delta x} \\ \frac{\sigma_i^{n+1} - \sigma_i^n}{\Delta t} &= \mu \frac{\nu_{i+1}^n - \nu_{i-1}^n}{2\Delta x} \end{aligned}$$

Equations to update the system:

$$\begin{aligned} \nu_i^{n+1} &= \nu_i^n + \frac{1}{\rho} \frac{\Delta t}{2\Delta x} (\sigma_{i+1}^n - \sigma_{i-1}^n) \\ \sigma_i^{n+1} &= \sigma_i^n + \mu \frac{\Delta t}{2\Delta x} (\nu_{i+1}^n - \nu_{i-1}^n) \end{aligned}$$

### 2.3.2 Leapfrog Scheme

$$\begin{aligned} \rho \frac{\nu_i^{n+1} - \nu_i^{n-1}}{2\Delta t} &= \frac{\sigma_{i+1}^n - \sigma_{i-1}^n}{2\Delta x} \\ \frac{\sigma_i^{n+1} - \sigma_i^{n-1}}{2\Delta t} &= \mu \frac{\nu_{i+1}^n - \nu_{i-1}^n}{2\Delta x} \end{aligned}$$

Equations to update the system:

$$\begin{aligned} \nu_i^{n+1} &= \nu_i^{n-1} + \frac{1}{\rho} \frac{\Delta t}{\Delta x} (\sigma_{i+1}^n - \sigma_{i-1}^n) \\ \sigma_i^{n+1} &= \sigma_i^{n-1} + \mu \frac{\Delta t}{\Delta x} (\nu_{i+1}^n - \nu_{i-1}^n) \end{aligned}$$

### 2.3.3 Lax-Wendroff Scheme

For stress:

$$\begin{aligned} \sigma_i^{n+1} &= \sigma_i^n + (\sigma_t)_i^n \Delta t + (\sigma_{tt})_i^n \frac{(\Delta t)^2}{2} \\ &= \sigma_i^n + \mu (\nu_x)_i^n \Delta t + \frac{\mu}{\rho} (\sigma_{xx})_i^n \frac{(\Delta t)^2}{2} \\ &= \sigma_i^n + \mu \left( \frac{\nu_{i+1}^n - \nu_{i-1}^n}{2\Delta x} \right) \Delta t + \frac{\mu}{\rho} \left( \frac{\sigma_{i+1}^n - 2\sigma_i^n + \sigma_{i-1}^n}{(\Delta x)^2} \right) \frac{(\Delta t)^2}{2} \end{aligned}$$


---

For velocity:

$$\begin{aligned}
\nu_i^{n+1} &= \nu_i^n + (\nu_t)_i^n \Delta t + (\nu_{tt})_i^n \frac{(\Delta t)^2}{2} \\
&= \nu_i^n + \frac{1}{\rho} (\sigma_x)_i^n \Delta t + \frac{\mu}{\rho} (\nu_{xx})_i^n \frac{(\Delta t)^2}{2} \\
&= \nu_i^n + \frac{1}{\rho} \left( \frac{\sigma_{i+1}^n - \sigma_{i-1}^n}{2\Delta x} \right) \Delta t + \frac{\mu}{\rho} \left( \frac{\nu_{i+1}^n - 2\nu_i^n + \nu_{i-1}^n}{(\Delta x)^2} \right) \frac{(\Delta t)^2}{2}
\end{aligned}$$

## 2.4 Mimetic Discretization

The mimetic discretization included here follows the approach described in []

$$\begin{aligned}
\nabla \sigma &= G \sigma \\
\nabla \cdot \nu &= D \nu
\end{aligned}$$

$$\begin{aligned}
\left( \frac{\partial \sigma}{\partial x} \right)_i &= \sum_{j=0}^{N+1} G_{ij} \sigma_j \quad i = 0, 1, \dots, N \\
\left( \frac{\partial \nu}{\partial x} \right)_i &= \sum_{j=0}^N D_{ij} \nu_j \quad i = 0, 1, \dots, N+1
\end{aligned}$$

Second order mimetic matrices: Gradient:

$$G = \frac{1}{\Delta x} \begin{bmatrix} -\frac{8}{3} & 3 & -\frac{1}{3} & & & & & \\ & -1 & 1 & & & & & \\ & & -1 & 1 & & & & \\ & & & \ddots & \ddots & & & \\ & & & & -1 & 1 & & \\ & & & & \frac{1}{3} & -3 & \frac{8}{3} & \end{bmatrix} \quad (4)$$

Extended Divergence:

$$D = \frac{1}{\Delta x} \begin{bmatrix} 0 & & & & & & & \\ -1 & 1 & & & & & & \\ & -1 & 1 & & & & & \\ & & \ddots & \ddots & & & & \\ & & & -1 & 1 & & & \\ & & & & & 0 & & \end{bmatrix} \quad (5)$$

Discretization in time is also staggered as described by the expressions:

$$\begin{aligned}
\sigma_i^n &= \sigma_i(n \Delta t) \\
\nu_i^{n+\frac{1}{2}} &= \nu_i \left( \left( n + \frac{1}{2} \right) \Delta t \right)
\end{aligned}$$

Thus the equations to update the system are:

$$\begin{aligned}
\nu_i^{n+\frac{1}{2}} &= \nu_i^{n-\frac{1}{2}} + \frac{\Delta t}{\rho} \sum_{j=0}^{N+1} G_{ij} \sigma_j^n \quad i = 0, 1, \dots, N \\
\sigma_i^{n+1} &= \sigma_i^{n-1} + \mu \Delta t \sum_{j=0}^N D_{ij} \nu_j^{n+\frac{1}{2}} \quad i = 0, 1, \dots, N+1
\end{aligned}$$

The discrete version of the boundary conditions:  $\sigma_0 = 0$  and  $\sigma_{N+1} = 0$  allows the elimination of the rows corresponding to:  $\frac{d\sigma_0}{dt}$  and  $\frac{d\sigma_{N+1}}{dt}$ .



---

### 3.3.1 Leapfrog Scheme

$$\begin{aligned}\frac{p_{ij}^{n+1} - p_{ij}^{n-1}}{2\Delta t} &= -K \left[ \left( \frac{u_{i+1j}^n - u_{i-1j}^n}{2\Delta x} \right) + \left( \frac{v_{ij+1}^n - v_{ij-1}^n}{2\Delta y} \right) \right] \\ \frac{u_{ij}^{n+1} - u_{ij}^{n-1}}{2\Delta t} &= -\frac{1}{\rho} \left( \frac{p_{i+1j}^n - p_{i-1j}^n}{2\Delta x} \right) \\ \frac{v_{ij}^{n+1} - v_{ij}^{n-1}}{2\Delta t} &= -\frac{1}{\rho} \left( \frac{p_{ij+1}^n - p_{ij-1}^n}{2\Delta y} \right)\end{aligned}$$

Equations to update the system:

$$\begin{aligned}p_{ij}^{n+1} &= p_{ij}^{n-1} - K \frac{\Delta t}{\Delta x} (u_{i+1j}^n - u_{i-1j}^n) - K \frac{\Delta t}{\Delta y} (v_{ij+1}^n - v_{ij-1}^n) \\ u_{ij}^{n+1} &= u_{ij}^{n-1} - \frac{1}{\rho} \frac{\Delta t}{\Delta x} (p_{i+1j}^n - p_{i-1j}^n) \\ v_{ij}^{n+1} &= v_{ij}^{n-1} - \frac{1}{\rho} \frac{\Delta t}{\Delta y} (p_{ij+1}^n - p_{ij-1}^n)\end{aligned}$$

### 3.3.2 Lax-Wendroff Scheme

For pressure:

$$\begin{aligned}p_{ij}^{n+1} &= p_{ij}^n + (p_t)_{ij}^n \Delta t + (p_{tt})_{ij}^n \frac{(\Delta t)^2}{2} \\ &= p_{ij}^n - K (u_x + v_y)_{ij}^n \Delta t + \frac{K}{\rho} (p_{xx} + p_{yy})_{ij}^n \frac{(\Delta t)^2}{2} \\ &= p_{ij}^n - K \left( \frac{u_{i+1j}^n - u_{i-1j}^n}{2\Delta x} \right) \Delta t - K \left( \frac{v_{ij+1}^n - v_{ij-1}^n}{2\Delta y} \right) \Delta t \\ &\quad + \frac{K}{\rho} \left( \frac{p_{i+1j}^n - 2p_{ij}^n + p_{i-1j}^n}{(\Delta x)^2} \right) \frac{(\Delta t)^2}{2} + \frac{K}{\rho} \left( \frac{p_{ij+1}^n - 2p_{ij}^n + p_{ij-1}^n}{(\Delta y)^2} \right) \frac{(\Delta t)^2}{2}\end{aligned}$$

For  $u$  ( $x$  component of velocity):

$$\begin{aligned}u_{ij}^{n+1} &= u_{ij}^n + (u_t)_{ij}^n \Delta t + (u_{tt})_{ij}^n \frac{(\Delta t)^2}{2} \\ &= u_{ij}^n - \frac{1}{\rho} (p_x)_{ij}^n \Delta t + \frac{K}{\rho} (u_{xx} + v_{yx})_{ij}^n \frac{(\Delta t)^2}{2} \\ &= u_{ij}^n - \frac{1}{\rho} \left( \frac{p_{i+1j}^n - p_{i-1j}^n}{2\Delta x} \right) \Delta t + \frac{K}{\rho} \left( \frac{u_{i+1j}^n - 2u_{ij}^n + u_{i-1j}^n}{(\Delta x)^2} \right) \frac{(\Delta t)^2}{2} \\ &\quad + \frac{K}{\rho} \left( \frac{(v_{i+1j+1}^n - v_{i-1j+1}^n) - (v_{i+1j-1}^n - v_{i-1j-1}^n)}{4(\Delta x)(\Delta y)} \right) \frac{(\Delta t)^2}{2}\end{aligned}$$

For  $v$  ( $y$  component of velocity):

$$\begin{aligned}v_{ij}^{n+1} &= v_{ij}^n + (v_t)_{ij}^n \Delta t + (v_{tt})_{ij}^n \frac{(\Delta t)^2}{2} \\ &= v_{ij}^n - \frac{1}{\rho} (p_y)_{ij}^n \Delta t + \frac{K}{\rho} (v_{yy} + u_{xy})_{ij}^n \frac{(\Delta t)^2}{2} \\ &= v_{ij}^n - \frac{1}{\rho} \left( \frac{p_{ij+1}^n - p_{ij-1}^n}{2\Delta y} \right) \Delta t + \frac{K}{\rho} \left( \frac{v_{ij+1}^n - 2v_{ij}^n + v_{ij-1}^n}{(\Delta y)^2} \right) \frac{(\Delta t)^2}{2} \\ &\quad + \frac{K}{\rho} \left( \frac{(u_{i+1j+1}^n - u_{i-1j+1}^n) - (u_{i+1j-1}^n - u_{i-1j-1}^n)}{4(\Delta x)(\Delta y)} \right) \frac{(\Delta t)^2}{2}\end{aligned}$$


---

---

### 3.4 Mimetic Discretization

A typical set of 2D grids for mimetic discretization is included in Figure 2. The system is discretized analogously to the one-dimensional case:

$$\begin{aligned}\nabla p &= G p \\ \nabla \cdot (u, v) &= D (u, v)\end{aligned}$$

Resulting in the following system:

$$\begin{aligned}\left[ \frac{\partial p}{\partial x}, \frac{\partial p}{\partial y} \right]_i &= \sum_{j=1}^{(N_x+2)N_y+2N_x} G_{ij} p_j \quad i = 1, \dots, (N_x+1)N_y + N_x(N_y+1) \\ \left( \frac{\partial u}{\partial x} + \frac{\partial v}{\partial y} \right)_i &= \sum_{j=1}^{(N_x+1)N_y+N_x(N_y+1)} D_{ij} w_j \quad i = 1, \dots, (N_x+2)N_y + 2N_x\end{aligned}$$

with:  $p$  vector of the scalar quantity (pressure) evaluated in the center of grid in Fig. 2(a) and  $w = [u|v]$ , vector of vectorial quantity (composition of velocities): first part of  $x$ -components and final part of  $y$  components. Velocities are evaluated in the positions indicated by the numbers in Fig. 2(b), in this example nodes 1-24 correspond to  $x$ -components of velocity and nodes 25-49 correspond to  $y$ -components.

Likewise, a staggered temporal discretization is used:

$$\begin{aligned}p_i^n &= p_i(n \Delta t) \\ w_i^{n+\frac{1}{2}} &= w_i \left( \left( n + \frac{1}{2} \right) \Delta t \right)\end{aligned}$$

Thus, the resulting equations to update the system are:

$$\begin{aligned}w_i^{n+\frac{1}{2}} &= w_i^{n-\frac{1}{2}} + \frac{\Delta t}{\rho} \sum_{j=1}^{(N_x+2)N_y+2N_x} G_{ij} p_j^n \quad i = 1, \dots, (N_x+1)N_y + N_x(N_y+1) \\ p_i^{n+1} &= p_i^{n-1} + K \Delta t \sum_{j=1}^{(N_x+1)N_y+N_x(N_y+1)} D_{ij} w_j^{n+\frac{1}{2}} \quad i = 1, \dots, (N_x+2)N_y + 2N_x\end{aligned}$$


---

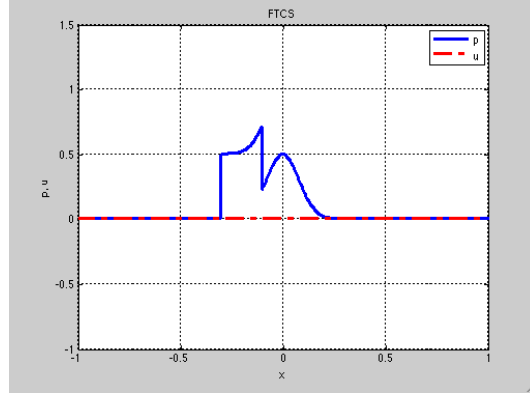


Figure 3: Acoustics 1D: Initial Condition

## 4 Results

### 4.1 1D Problems

#### 4.1.1 Acoustic Equations 1D

System of equations, constants, boundary conditions and initial values taken from [4].

$$p_t + K u_x = 0 \quad (8)$$

$$u_t + \frac{1}{\rho} p_x = 0 \quad (9)$$

with:  $u$ , velocity;  $p$ , pressure and constants:  $K = 0.25$  (Bulk Modulus of Compressibility) and  $\rho = 1$  (density). Domain:  $-1 \leq x \leq 1$ . Boundary conditions: solid walls. Initial condition:

$$\text{IC} \begin{cases} p(x, 0) = \frac{1}{2} \exp(-80x^2) + S(x) \\ u(x, 0) = 0 \end{cases}$$

with:

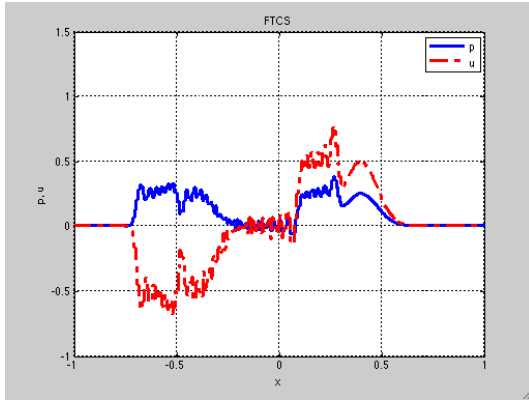
$$S(x) = \begin{cases} 0.5 & -0.3 < x < 0.1 \\ 0 & \text{otherwise} \end{cases}$$

Figure 3 displays the initial condition studied for the one-dimensional system of acoustic equations. As can be noted at different time steps in Figures 4-6 a direct implementation of boundary conditions (velocity and pressure equal to zero in left and right walls) render the FD schemes unusable for times greater than the bouncing with the walls. Figures 7-9 show that once the numerical boundary conditions are adjusted to ‘adequate’ values, the FD schemes produce accurate results. Mimetic discretizations are virtually free of this tuning procedure and this type of Dirichlet boundary conditions can be incorporated directly without affecting the functioning of the scheme. (In the latter figures, the mimetic results are just included for comparison, and correspond to the former figures). From the pictures it is clear that the FTCS scheme does not produce good results. All the results shown correspond to a grid of 500 cells and  $\Delta t = \Delta x/c$ ,  $c = \sqrt{(K/\rho)}$ .

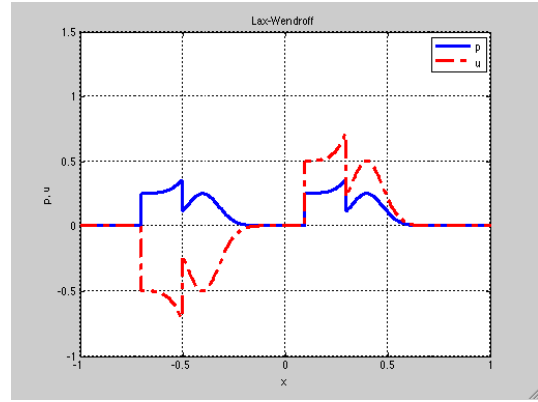
The analytical solution for this problem (before bouncing with the walls) can be calculated through the following equations:

$$u(x, t) = -\frac{1}{2Z_0} [p^\circ(x + c_0t) - p^\circ(x - c_0t)] + \frac{1}{2} [u^\circ(x + c_0t) + u^\circ(x - c_0t)] \quad (10)$$

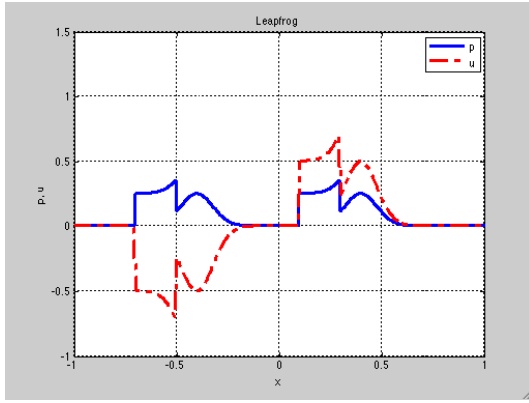
$$p(x, t) = \frac{1}{2} [p^\circ(x + c_0t) + p^\circ(x - c_0t)] - \frac{Z_0}{2} [u^\circ(x + c_0t) - u^\circ(x - c_0t)] \quad (11)$$



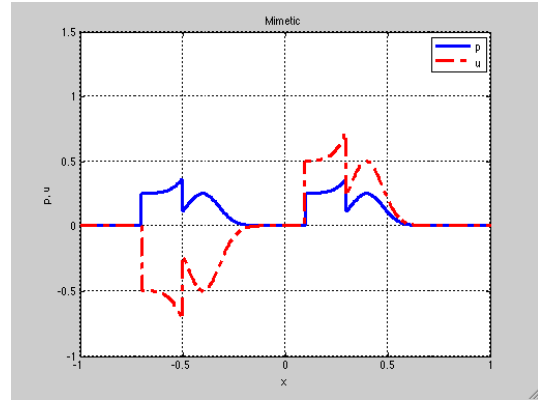
(a) FTCS



(b) Lax-Wendroff



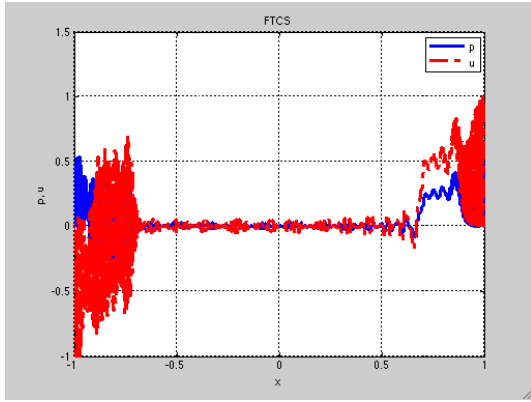
(c) Leapfrog



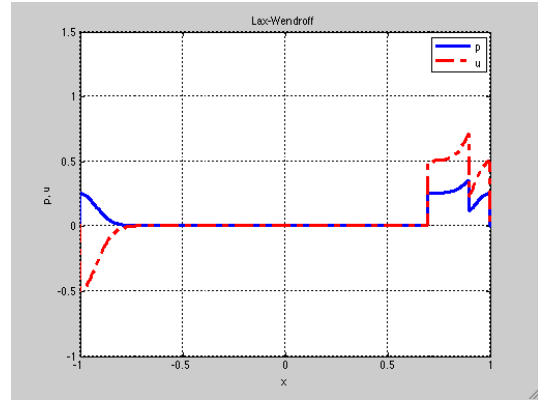
(d) Mimetic

Figure 4: Acoustics 1D:  $t = 0.8$  - Naive Numeric Boundary Conditions

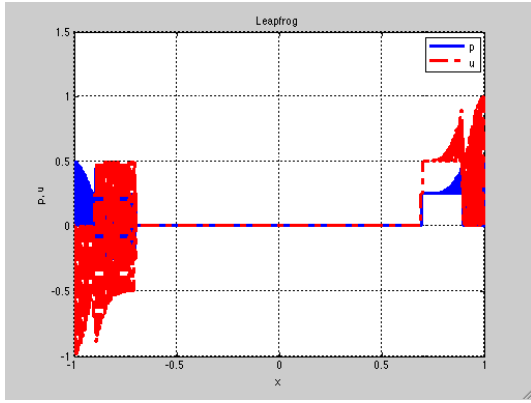




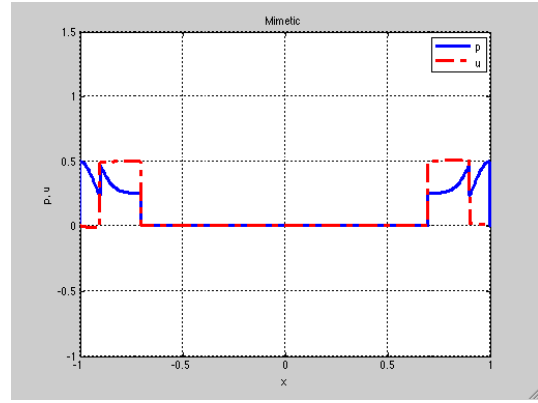
(a) FTCS



(b) Lax-Wendroff

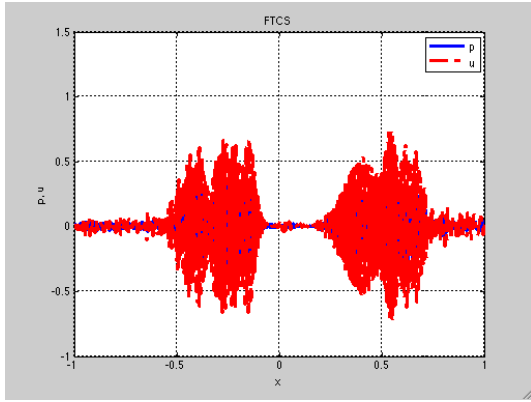


(c) Leapfrog

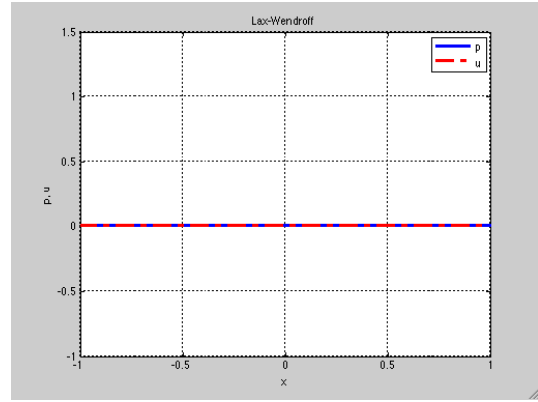


(d) Mimetic

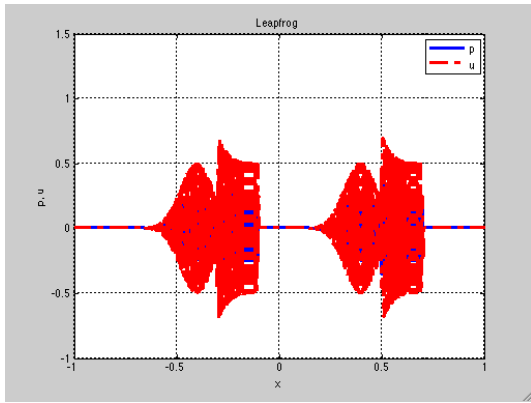
Figure 5: Acoustics 1D:  $t = 2$  - Naive Numeric Boundary Conditions



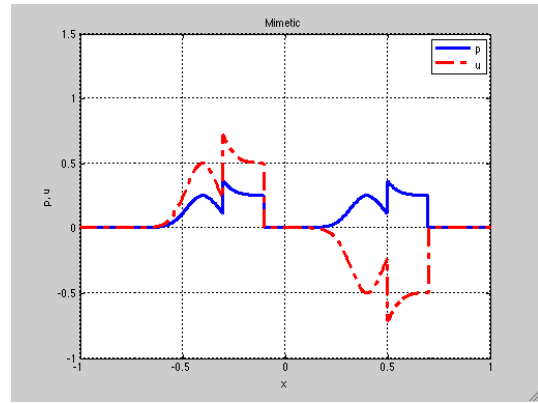
(a) FTCS



(b) Lax-Wendroff

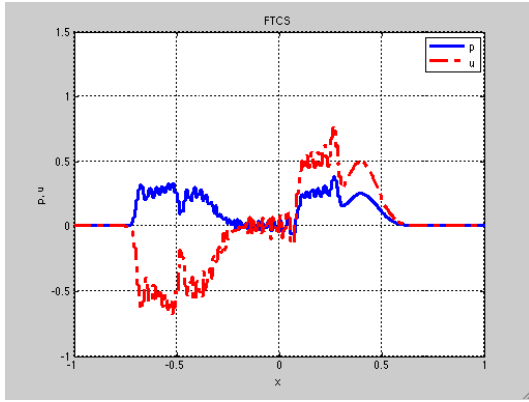


(c) Leapfrog

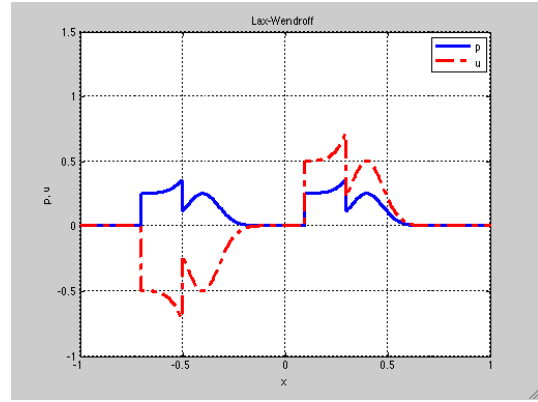


(d) Mimetic

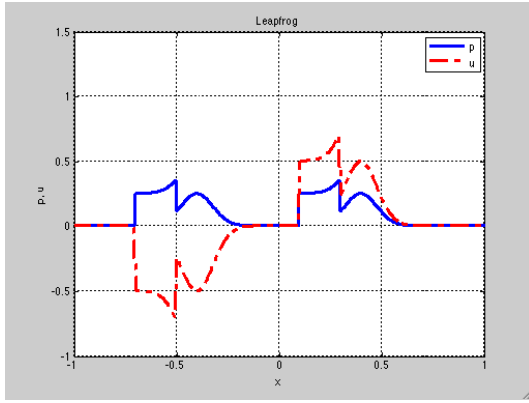
Figure 6: Acoustics 1D:  $t = 3.2$  - Naive Numeric Boundary Conditions



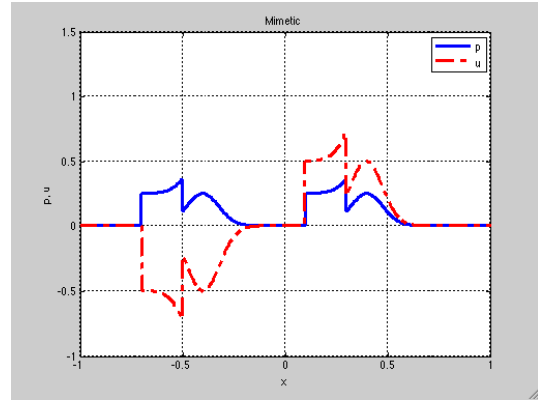
(a) FTCS



(b) Lax-Wendroff

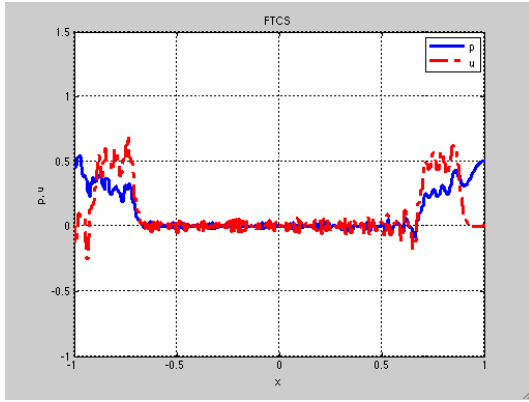


(c) Leapfrog

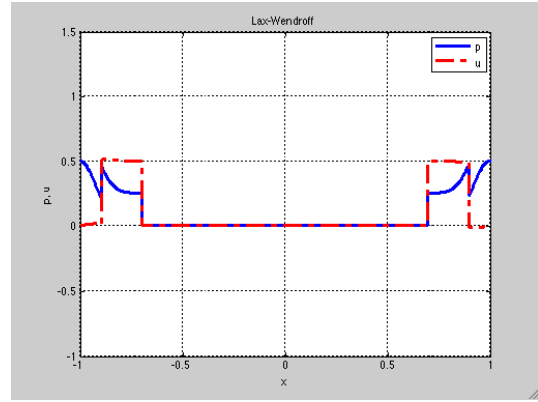


(d) Mimetic

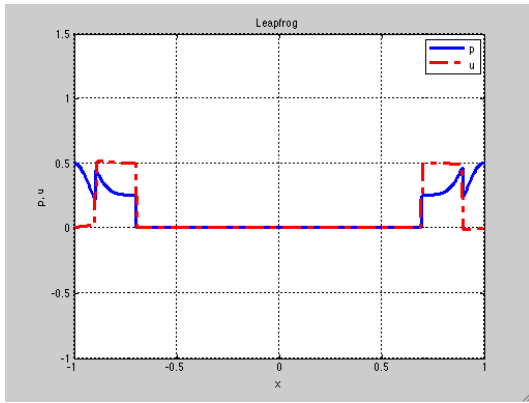
Figure 7: Acoustics 1D:  $t = 0.8$  - Numeric Boundary Conditions Adjusted for FD



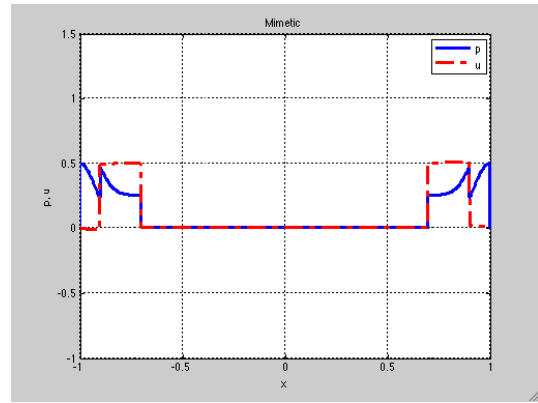
(a) FTCS



(b) Lax-Wendroff

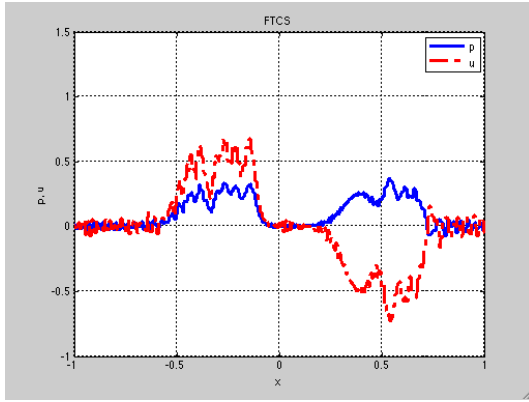


(c) Leapfrog

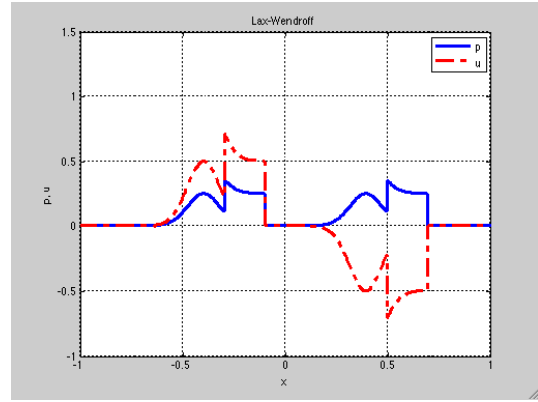


(d) Mimetic

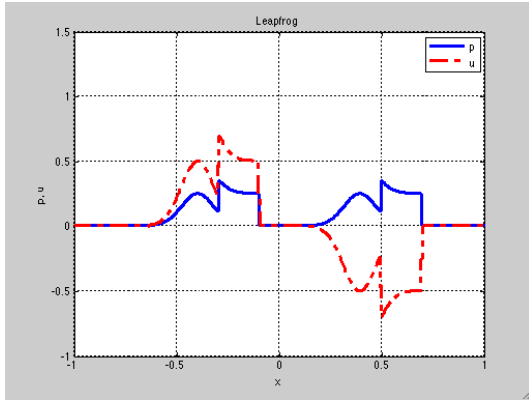
Figure 8: Acoustics 1D:  $t = 2$  - Numeric Boundary Conditions Adjusted for FD



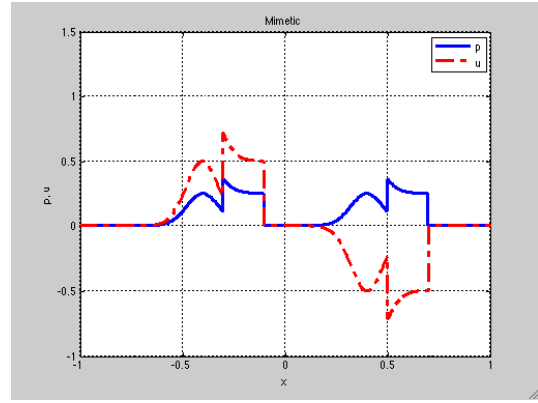
(a) FTCS



(b) Lax-Wendroff



(c) Leapfrog



(d) Mimetic

Figure 9: Acoustics 1D:  $t = 3.2$  - Numeric Boundary Conditions Adjusted for FD

---

with:  $c_0 = \sqrt{(K/\rho)}$ ,  $Z_0 = \rho c_0$ , and  $p^\circ(x)$  and  $u^\circ(x)$  corresponding to the initial condition [4]. Hence, for this example, results are evaluated using the following error grid function norm:

$$\|\mathbf{E}\|_2 = \left[ h \sum_{i=1}^N |e_i| \right]^{\frac{1}{2}} \quad (12)$$

In the case of velocity:  $e_i = U(x_i) - u(x_i)$ , with  $U$  representing the analytical solution, eq. (10), and  $u$  the numerical solution, while in the case of pressure  $e_i = P(x_i) - p(x_i)$ , with  $P$  representing the analytical solution, eq. (11), and  $p$  the numerical solution. Table 1 and Table 2 include errors (grid function norm) while Figure 10 displays the logarithmic plot of the errors vs. different  $\Delta x$ . These error calculations agree with the behavior seen in previous plots.

Table 1: Error (grid function norm) for Acoustic 1D - pressure ( $p$ )

$\Delta x$	FTCS	Lax-Wendroff	Leapfrog	Mimetic
$2.00 \times 10^{-2}$	$7.6730 \times 10^{-2}$	$5.0000 \times 10^{-2}$	$5.0000 \times 10^{-2}$	$1.1318 \times 10^{-10}$
$1.00 \times 10^{-2}$	$6.0763 \times 10^{-2}$	$3.5355 \times 10^{-2}$	$3.5355 \times 10^{-2}$	$9.0881 \times 10^{-11}$
$5.00 \times 10^{-3}$	$4.6763 \times 10^{-2}$	$2.5000 \times 10^{-2}$	$2.5000 \times 10^{-2}$	$7.6468 \times 10^{-11}$
$2.50 \times 10^{-3}$	$3.6385 \times 10^{-2}$	$1.7678 \times 10^{-2}$	$1.7678 \times 10^{-2}$	$6.7710 \times 10^{-11}$
$1.25 \times 10^{-3}$	$2.9604 \times 10^{-2}$	$1.2500 \times 10^{-2}$	$1.2500 \times 10^{-2}$	$6.2748 \times 10^{-11}$
$6.25 \times 10^{-4}$	$2.3324 \times 10^{-2}$	$8.8388 \times 10^{-3}$	$8.8388 \times 10^{-3}$	$6.0079 \times 10^{-11}$

Table 2: Error (grid function norm) for Acoustic 1D - velocity ( $u$ )

$\Delta x$	FTCS	Lax-Wendroff	Leapfrog	Mimetic
$2.00 \times 10^{-2}$	$1.6828 \times 10^{-1}$	$1.0000 \times 10^{-1}$	$1.0000 \times 10^{-1}$	$9.3561 \times 10^{-11}$
$1.00 \times 10^{-2}$	$1.3092 \times 10^{-1}$	$7.0711 \times 10^{-2}$	$7.0715 \times 10^{-2}$	$1.0861 \times 10^{-10}$
$5.00 \times 10^{-3}$	$9.9415 \times 10^{-2}$	$5.0000 \times 10^{-2}$	$5.0001 \times 10^{-2}$	$1.1300 \times 10^{-10}$
$2.50 \times 10^{-3}$	$7.6162 \times 10^{-2}$	$3.5355 \times 10^{-2}$	$3.5355 \times 10^{-2}$	$1.1414 \times 10^{-10}$
$1.25 \times 10^{-3}$	$6.0345 \times 10^{-2}$	$2.5000 \times 10^{-2}$	$2.5000 \times 10^{-2}$	$1.1443 \times 10^{-10}$
$6.25 \times 10^{-4}$	$4.7912 \times 10^{-2}$	$1.7678 \times 10^{-2}$	$1.7678 \times 10^{-2}$	$1.1450 \times 10^{-10}$

#### 4.1.2 Shallow Water Equations 1D

System of equations, constants, boundary conditions and initial values taken from [3].

$$\eta_t + H u_x = 0 \quad (13)$$

$$u_t + g \eta_x = 0 \quad (14)$$

with:  $u$ , velocity;  $\eta$ , level of perturbation and constants:  $H = 10$  (Depth) and  $g = 9.81$  (gravity). Domain:  $0 \leq x \leq 1$ . Boundary conditions: left, an oscillating wall with constant input equal to 0.3 and right, a solid wall. Initial condition:

$$\text{IC} \begin{cases} \eta(x, 0) = 0 \\ u(x, 0) = 0 \end{cases}$$

Figure 11 displays the initial condition studied for the one-dimensional system of shallow water. Just as in the previous example, a direct implementation of boundary conditions (velocity equal to 0.3 in left wall and zero in right wall and pressure equal to zero in left and right walls) render the FD schemes unusable (Fig. 12-14) and some adjustment has to be done to make them work for times greater than the bouncing

---

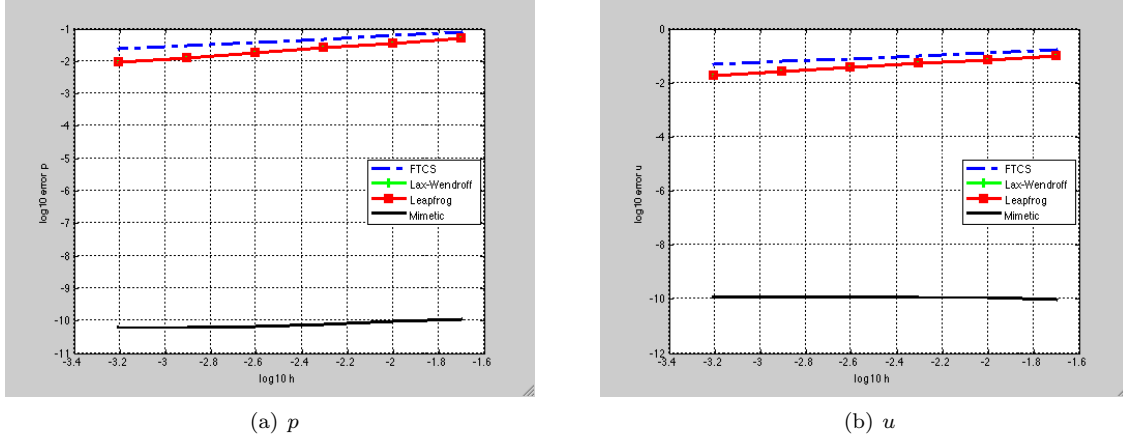


Figure 10: Acoustic 1D: Error (grid function norm)

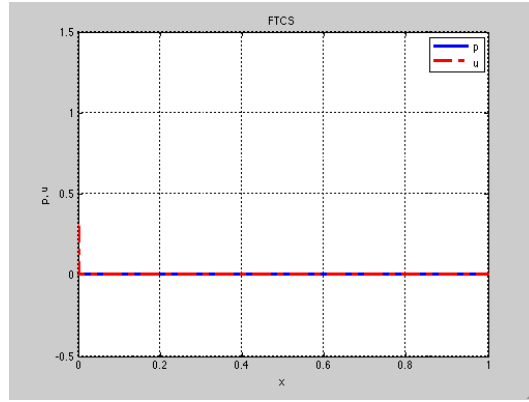


Figure 11: Shallow Water 1D: Initial Condition

with the walls (Fig. 15-17). Mimetic discretization works with the direct specification of the boundary conditions. Again, FTCS scheme produce poor oscillatory results. All the results shown correspond to a grid of 200 cells and  $\Delta t = \Delta x/c$ ,  $c = \sqrt{Hg}$ .

#### 4.1.3 Burgers' Equation for Inviscid Flow

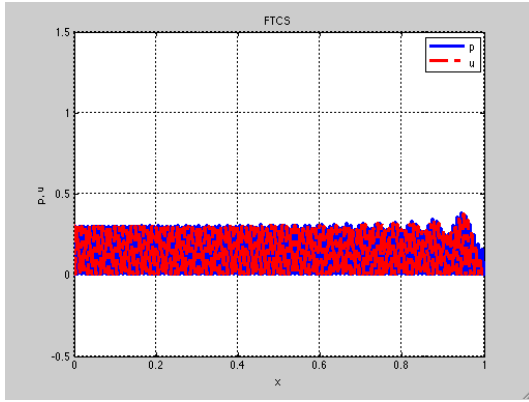
Equation, boundary conditions and initial values taken from [5].

$$\begin{aligned} \frac{\partial u}{\partial t} + \frac{\partial f(u)}{\partial x} &= 0 \\ u_t + \left( \frac{1}{2} u^2 \right)_x &= 0 \end{aligned}$$

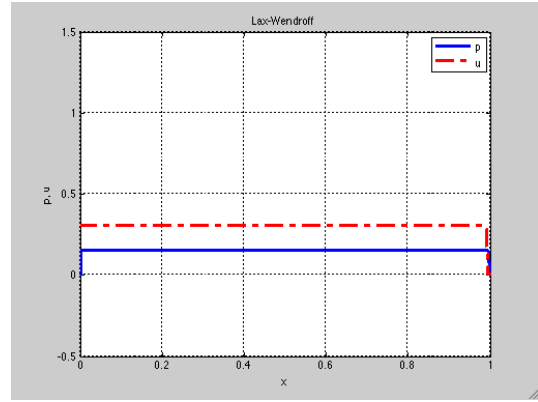
with:  $u$ , velocity. Domain:  $0 \leq x \leq 1$ . Boundary conditions: open. Initial condition:

$$u(x, 0) = \exp[-10(4x - 1)^2]$$

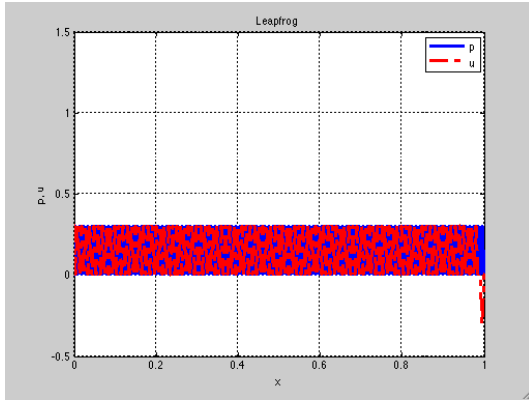
Figure 18 displays the initial condition studied for the Burgers' Equation for inviscid flow. This example is interesting because it corresponds to a nonlinear equation, that develops a shock front. Figures 19-21 display results at different times for a grid of 500 cells and  $\Delta t = \Delta x$ . It can be observed that all the methods tend to produce reasonable results around the shock front although Lax-Wendroff seems to have a greater overshoot in some time steps.



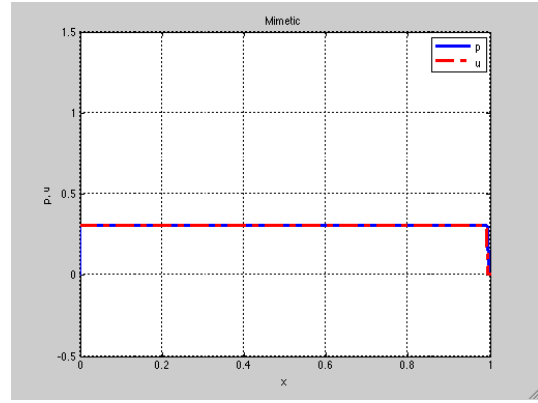
(a) FTCS



(b) Lax-Wendroff



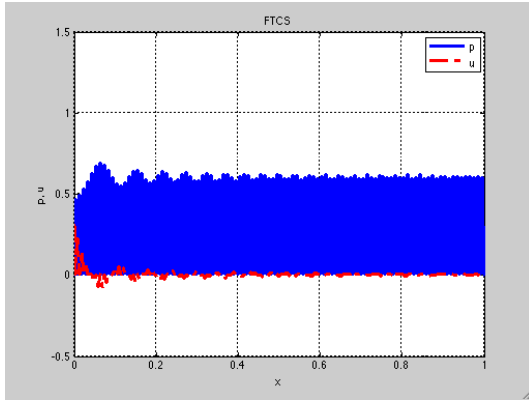
(c) Leapfrog



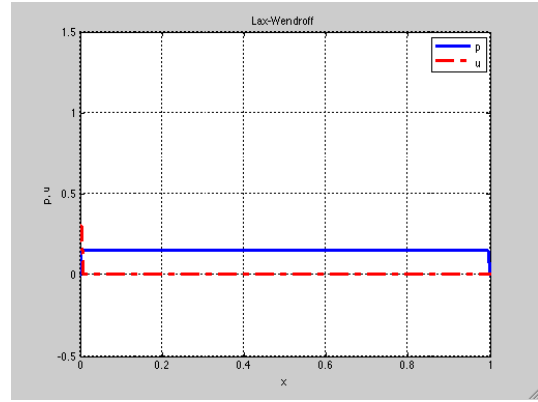
(d) Mimetic

Figure 12: Shallow Water 1D:  $t = 0.1005$  - Naive Numeric Boundary Conditions

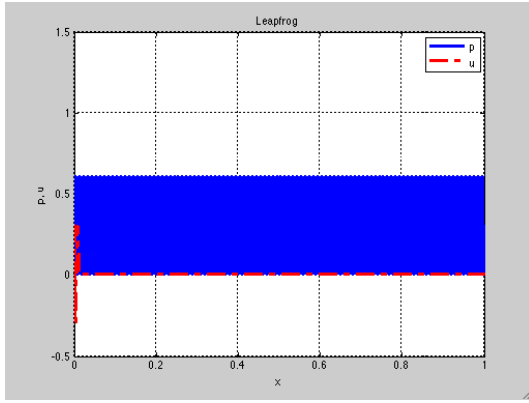




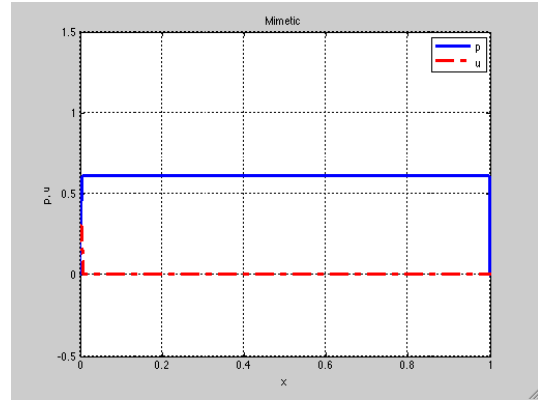
(a) FTCS



(b) Lax-Wendroff

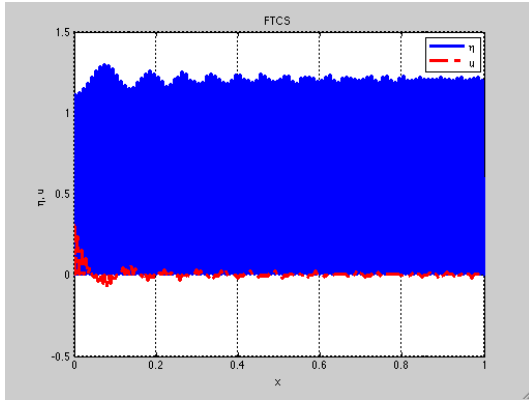


(c) Leapfrog

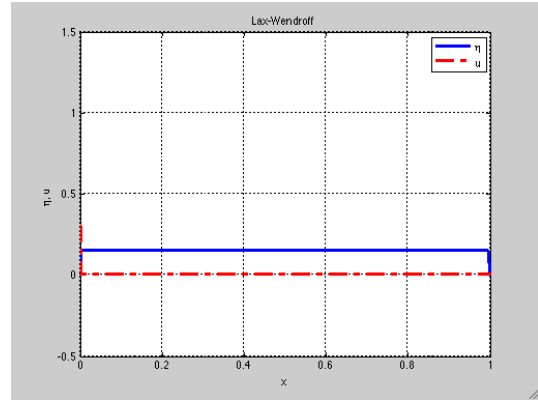


(d) Mimetic

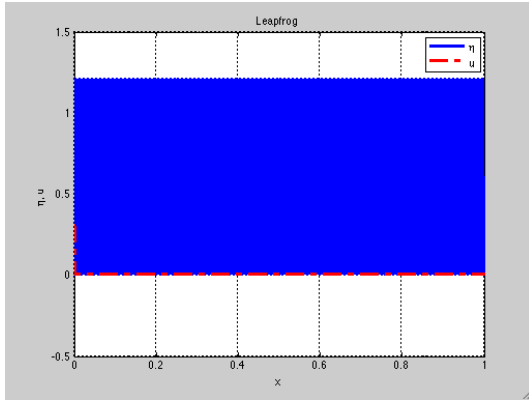
Figure 13: Shallow Water 1D:  $t = 0.2014$  - Naive Numeric Boundary Conditions



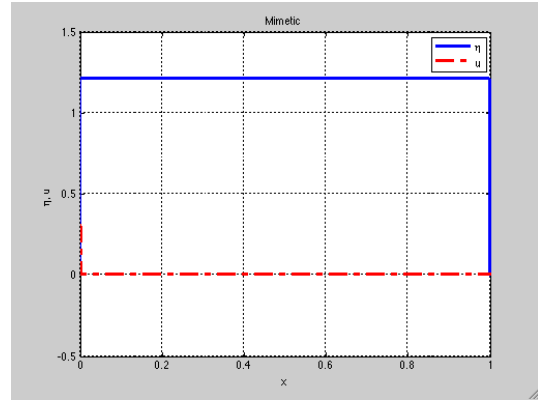
(a) FTCS



(b) Lax-Wendroff

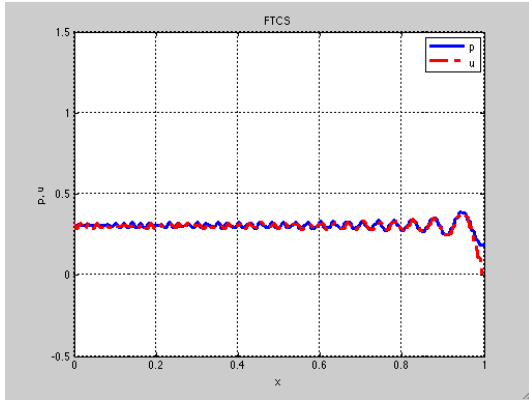


(c) Leapfrog

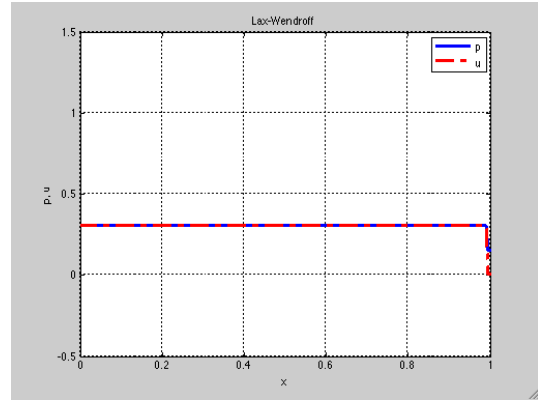


(d) Mimetic

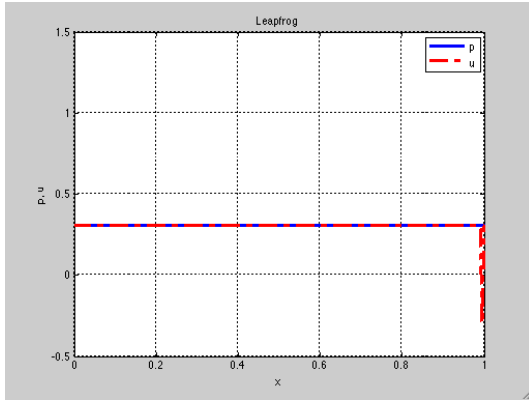
Figure 14: Shallow Water 1D:  $t = 0.4039$  - Naive Numeric Boundary Conditions



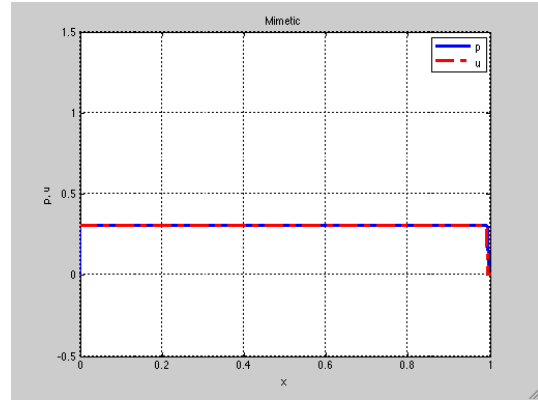
(a) FTCS



(b) Lax-Wendroff

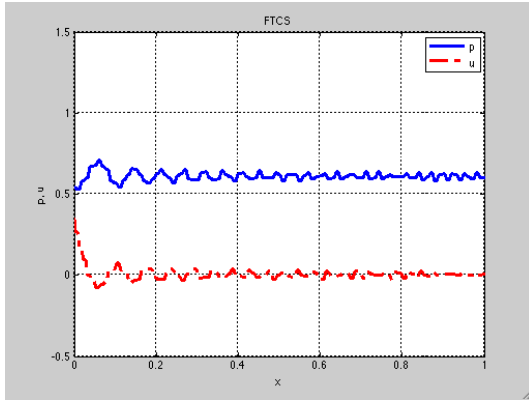


(c) Leapfrog

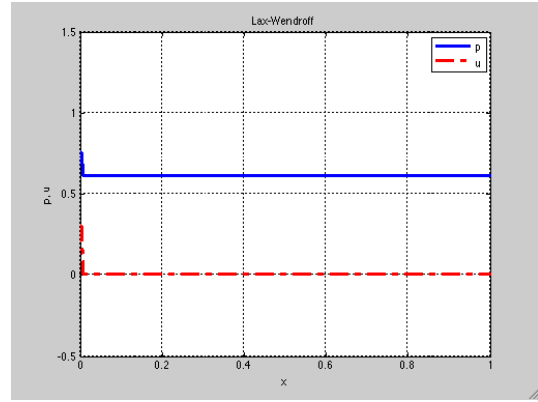


(d) Mimetic

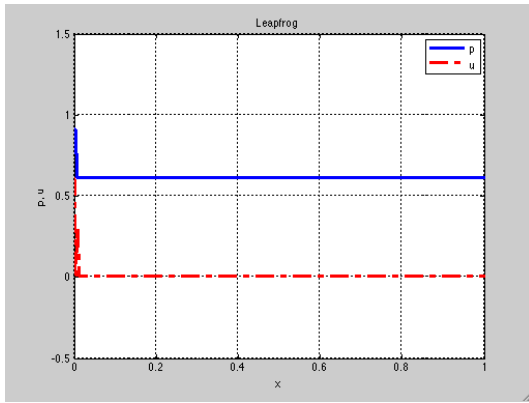
Figure 15: Shallow Water 1D:  $t = 0.1005$  - Numeric Boundary Conditions Adjusted for FD



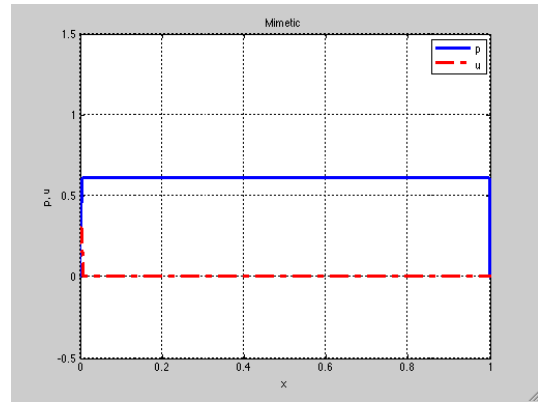
(a) FTCS



(b) Lax-Wendroff

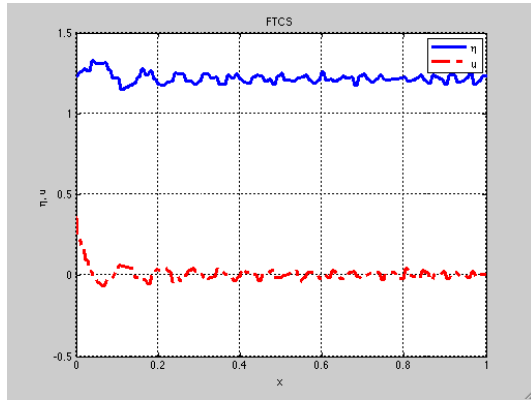


(c) Leapfrog

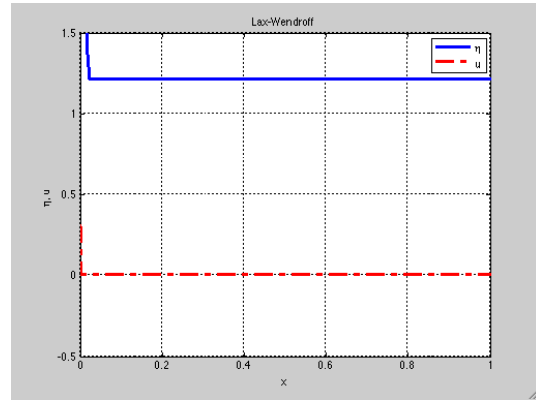


(d) Mimetic

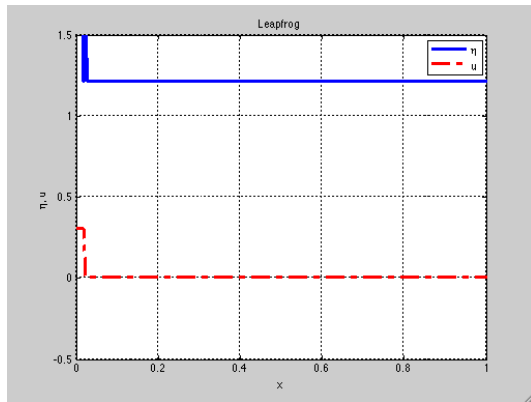
Figure 16: Shallow Water 1D:  $t = 0.2014$  - Numeric Boundary Conditions Adjusted for FD



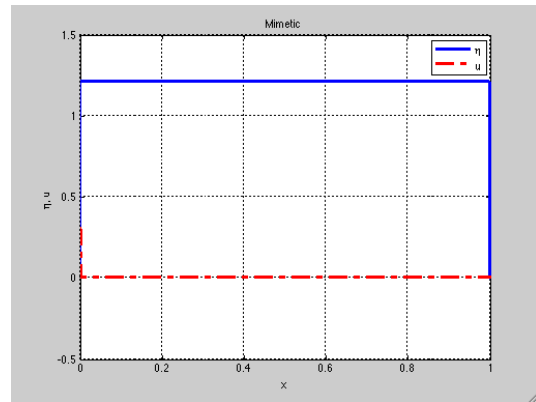
(a) FTCS



(b) Lax-Wendroff



(c) Leapfrog



(d) Mimetic

Figure 17: Shallow Water 1D:  $t = 0.4039$  - Numeric Boundary Conditions Adjusted for FD

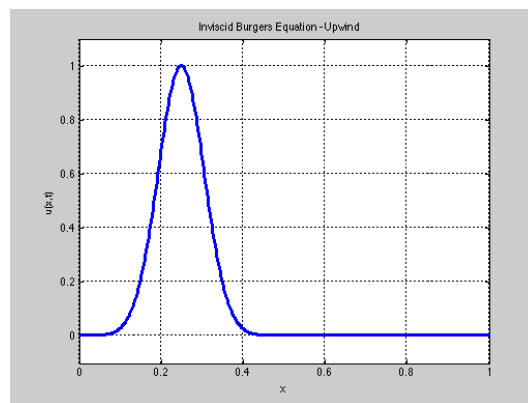
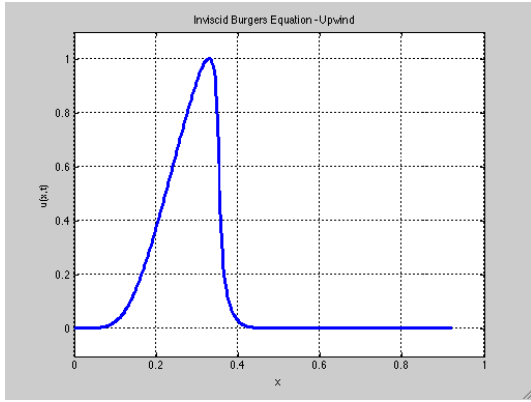
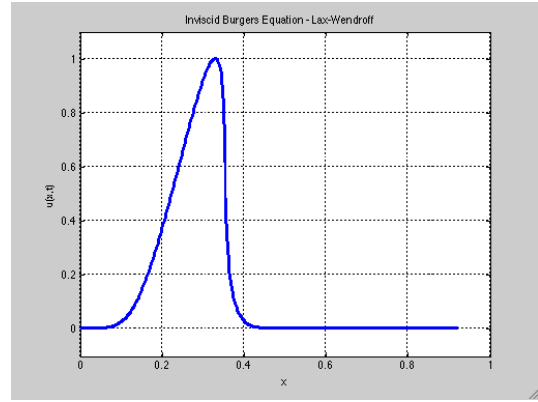


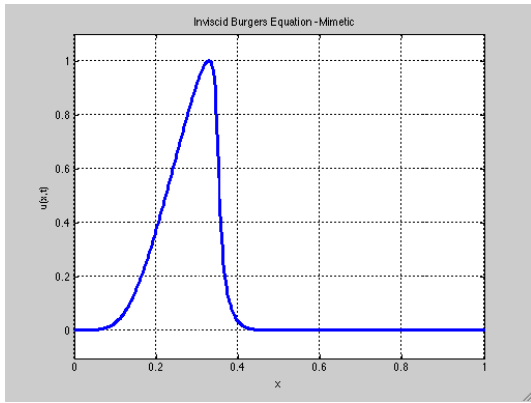
Figure 18: Inviscid Burgers' Equation: Initial Condition



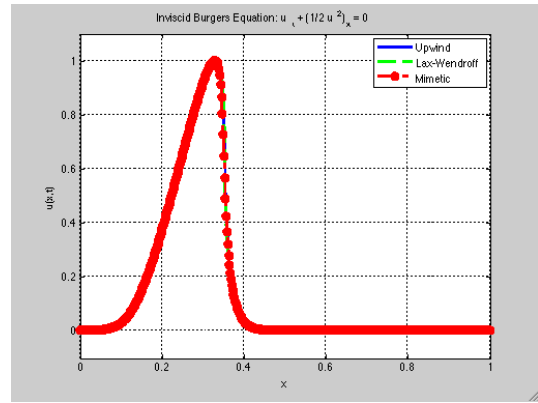
(a) Upwind



(b) Lax-Wendroff

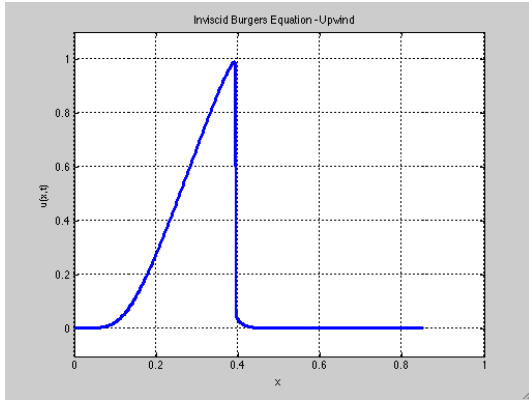


(c) Mimetic

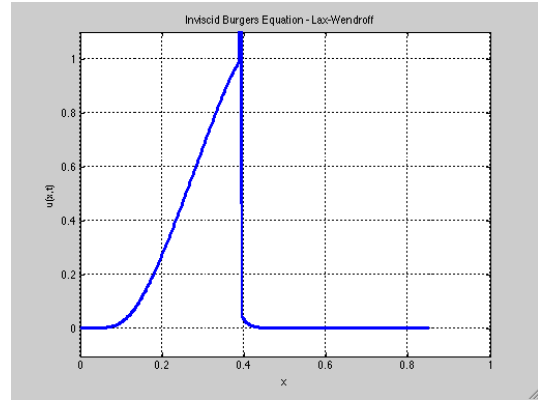


(d) Superposition

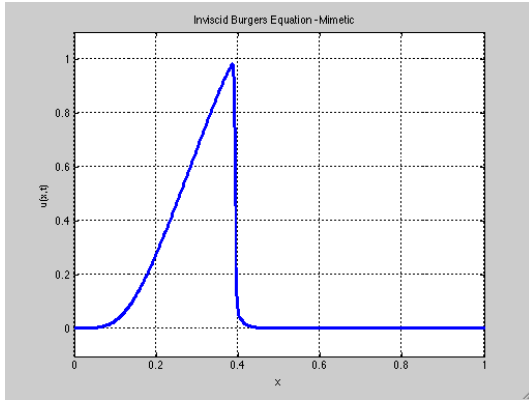
Figure 19: Inviscid Burgers' Equation:  $t = 0.08$



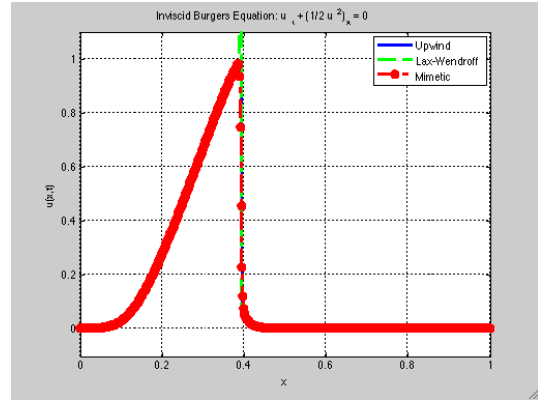
(a) Upwind



(b) Lax-Wendroff

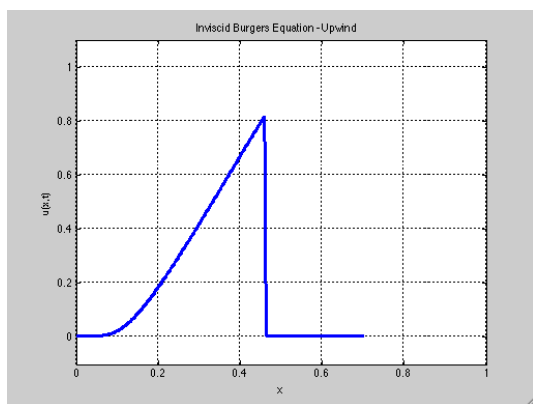


(c) Mimetic

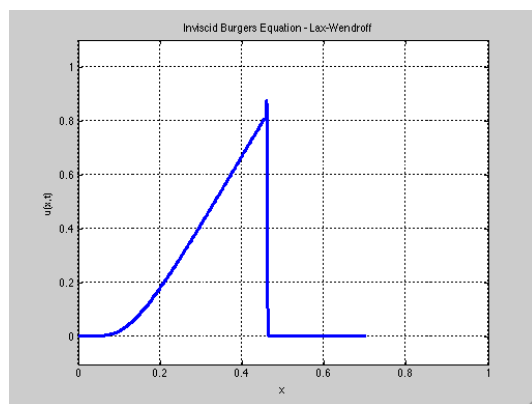


(d) Superposition

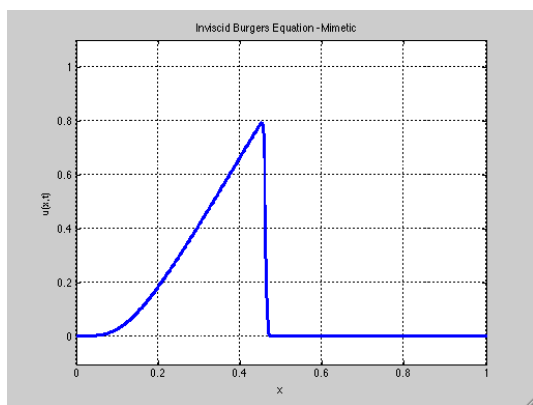
Figure 20: Inviscid Burgers' Equation:  $t = 0.15$



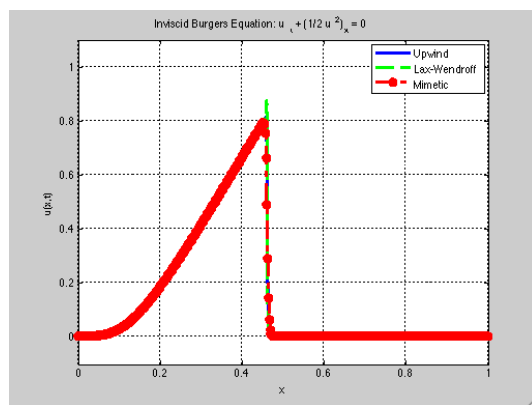
(a) Upwind



(b) Lax-Wendroff



(c) Mimetic



(d) Superposition

Figure 21: Inviscid Burgers' Equation:  $t = 0.3$